

RARE EARTH ELEMENT GEOCHEMISTRY OF MESOARCHEAN QUARTZITES OF GHATTIHOSAHALLI SCHIST BELT, WESTERN DHARWAR CRATON, KARNATAKA, INDIA: IMPLICATIONS ON PROVENANCE, PALEO-WEATHERING AND TECTONIC SETTING

M. VINAYA

Research Scholar, Department of PG Studies and Research in Applied Geology, Kuvempu University, Jnana Sahyadri, Shankaraghatta, Karnataka, India. Email: vinaym.vinu5@gmail.com

GOVINDARAJU *

Professor, Department of PG Studies and Research in Applied Geology, Kuvempu University, Jnana Sahyadri, Shanakaraghatta, Karnataka, India. *Corresponding Author Email: drgov@yahoo.com
ORCID ID: 0000-0002-0119-4826

G. S. SOMESHA

Lecturer, Department of PG Studies and Research in Applied Geology, Kuvempu University, Jnana Sahyadri, Shanakaraghatta, Karnataka, India. Email: somesh.g.shivu@gmail.com

Abstract

The present study explores and characterizes the quartzites from the Ghattihosahalli Schist Belt for major and trace elements, including REEs, in order to analyze their paleo-weathering and provenance characteristics, as well as possible tectonic settings. A petrography and geochemical analysis of the quartzite was conducted in order to determine the extent of paleo-weathering and its provenance. Geochemical data plots like $\log(\text{SiO}_2/\text{Al}_2\text{O}_3)$ vs. $\log(\text{Fe}_2\text{O}_3/\text{K}_2\text{O})$ & $\log(\text{SiO}_2/\text{Al}_2\text{O}_3)$ vs. $\log(\text{Na}_2\text{O}/\text{K}_2\text{O})$ categorize the quartzites as sub-arkose to sub-litharenite and fuchsite quartzites as arkose to litharenite. Na_2O vs. K_2O plot diagram shows quartz abundance in studied samples. Quartzite exhibits moderate to intense chemical weathering based on CIW, CIA, PIA and A-CN-K plots, while fuchsite quartzite exhibits semi-arid to semi-humid conditions. Chondrite normalized REE are fractionated in fuchsite quartzites and quartzites with low HREE. Discriminant functions suggest that studied samples have been formed in quartzose sedimentary fields. Plotting TiO_2 vs. Ni indicates felsic provenance for the samples. $\text{Al}_2\text{O}_3/\text{SiO}_2$ vs. $\text{Fe}_2\text{O}_3+\text{MgO}$ and SiO_2 vs. $\text{K}_2\text{O}/\text{Na}_2\text{O}$ plots indicate quartzites occupied a passive margin tectonic setting. The major and trace element ratios, patterns of REE normalized on chondrites and diagrams of normalized multi-elements depicts that the studied quartzites are predominantly felsic with some mafic contribution.

Index Terms: Geochemistry, Provenance, Paleo-Weathering, Quartzites, REE, Tectonic Setting.

1. INTRODUCTION

The importance of sedimentary geochemistry has gained wide recognition in recent years for its role in understanding clastic sedimentary suite evolution, provenance, and source weathering. It has been shown in numerous studies that the chemical composition of the clastic sedimentary rocks is influenced by a variety of factors, including the composition of the source rock, the extent and duration of weathering, the method of transportation, and post-depositional processes, such as diagenesis. According to Bhatia and Crook [1]; Roser and Korsch [2], the geochemical studies have revealed that ancient sediments were deposited in tectonic settings. Considering the relatively small fractionation of rare

earth elements and immobile trace elements by sedimentary processes and low grade metamorphism, sediments are important indicators of the chemical composition of source rocks [3], [4]. Further, Nesbitt and Young [5] and Fedo et al [6], have demonstrated that the abundance of mobile elements may provide insights into ancient weathering regimes, paleo environmental conditions, and other chemical processes that sediments and their sources may have undergone in the past. The Archaean greenstone belt in the Indian shield, sedimentary successions with clastic sedimentary rocks play an important role. The greenstone belts of the Archean ages of the Dharwar Craton in South India allows us to examine how an early sedimentary system evolved during a critical period in earth's history [7]. As part of this study, we have attempted to understand the provenance, weathering condition, tectonic setting of quartzites from the Ghattihosahalli schist belt of western Dharwar craton, as well as the geochemistry of major, trace and rare earth elements, thus attempting to constrain the composition of the source rocks as well as the sedimentary setting.

2. GEOLOGICAL SETTINGS

The Ghattihosahalli schist belt (GHSB) is located on the western margin of the main Chitradurga schist belt in Karnataka. The supracrustal belt in this area is one of the best preserved in the state. This belt has a northwest trend and is linear. In the north, the belt stretches for over 25 km, and in the south, it extends east of Talya for over 25 km. On the west GHSB, the TTG Peninsular gneisses 3.1 Ga older than the belt [8] are poorly defined, and on the east, the old Chitradurga belt 2.6 Ga older than the belt [9]. Radhakrishna and Sreenivasaiah [10] describe the volcanic-sedimentary sequence as composed of ultramafic komatiites and amphibolites interlayered with fuchsite quartzite and barite. Viswanatha et al [11] reported the first record of spinifex texture in India from the serpentinite of this belt. The idealized upward stratigraphy of amphibolite, ultramafite and fuchsite quartzite visualized for this belt by Narayana and Naqvi [12] is not borne out by field evidences. The gneisses around the belt have abundant enclaves of amphibolites and ultramafic rocks. Two major geological components can be found within the schist belt. It was found in the western part of the area that the older components were found, which belong to the Sargur group. The Bababudan group has younger components on the eastern side of the belt, which make up the lower part of the Dharwar Supergroup. The Sargur supracrustals within the Ghattihosahalli belt are primarily composed of meta-ultramafics, mafics, and their associated subordinate metasediments arranged without stratigraphic distinction. As part of Ghattihosahalli belt, the Sargur complex exhibits a variety of metasediments associated with mafic and ultramafic rocks. Although the belt is composed of 10-15% metasedimentary rocks, its association with sub-aqueous volcanic rocks is very important for understanding Archaean sedimentation and volcanism [38]. The baryte occurs as thin lenses and bands of conformable but discontinuous structures within the quartzite near the metabasic and metaultramafic rocks underneath. Chromiferous quartzite is the predominant horizon in which barite bands occur. It is clear from the association of the metasediments in the field with the underlying mafic-ultramafic flows as well as their petrographic characteristics that the metasediments are volcanic exhalates [13].

3. STUDY AREA

The Ghattihosahalli schist belt in Chitradurga taluk of the Chitradurga district, which is part of the peninsular gneiss basement, is situated to the west of the younger Chitradurga greenstone belt, Dharwar Supergroup. The rectangular area (Fig. 1) covers an area about 341Sq kms and it forms the part of Survey of India toposheets No.:57 B/4, 57 B/8, 57 C/1 and C/5.

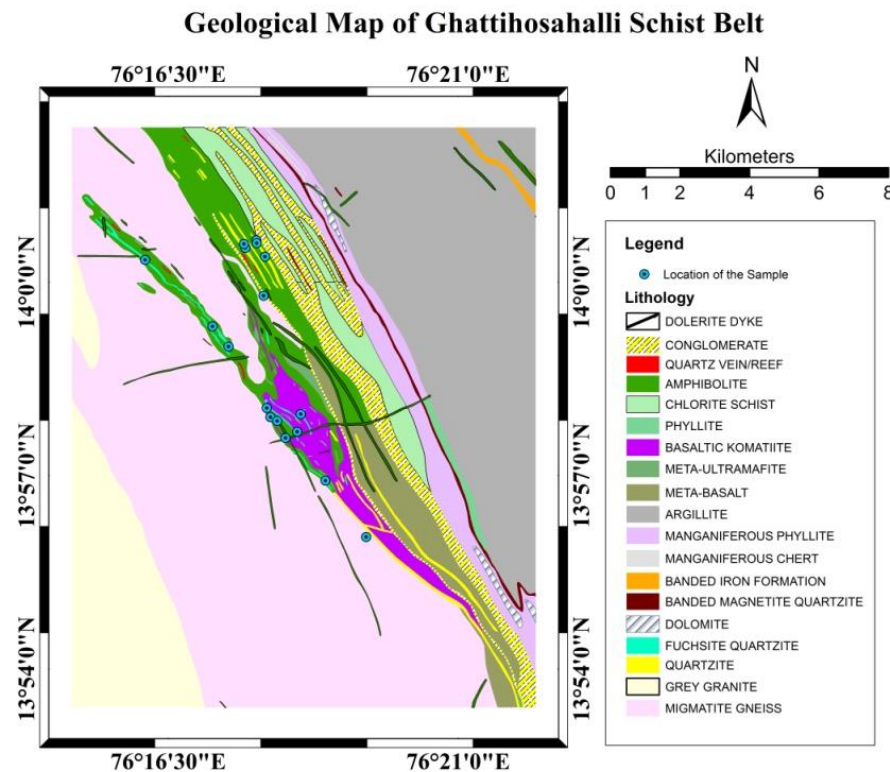


Fig 1: The Geological map of the study area with sample location (Adopted from Bhukosh, GSI portal 2023)

4. MATERIALS AND METHODS

In order to conduct the research, desk studies, geological field mapping, sampling and geochemical analyses were employed. For the purpose of conducting this study, geological mapping was conducted at a scale of 1: 25,000. A random sample of big, fresh, representative rocks from the field was collected for thin section analysis and geochemical analysis. The major oxides of 15 samples were identified and analyzed by using an XRF system from Bruker-AXS, Germany, equipped with a 4kW high power X-ray Rh anode tube (60 kV, 170 mA) and by using standard procedures at the Wadia Institute of Himalayan Geology, Dehradun, the SCIEX quadrupole type ICPMS 96, ELAN DRC-e to analyze trace and REEs. The precision & accuracy of the analysis are within the error levels of 5% and 10%, respectively, for major and trace analysis.

5. GEOLOGICAL OCCURRENCE

5.1 Quartzite

Quartzite from the sargur group in Ghattihosahalli belt occur inter layered with serpentized ultramafic rocks. They are well exposed in the Ghattihosahalli and kumminghatta village. In the quartzite layer, the sample collected is white to grayish in color, medium to coarse in size, and consists primarily of quartz, muscovite, opaque minerals, and kyanite, apatite, zircon, monazite, and xenotime in minor amounts. The rock is associated baryte, located within a km SSE of Ghattihosahalli village in which baryte interbedded with fuchsite quartzite (Fig. 2a) predominantly composed of quartz and fuchsite mica. There is an interstratification of barite with the fuchsite quartzites. The barite beds occur within mica schists and quartzites subparallel to the monocline structure. A Quartzite from old worked quarry pit (Fig. 2b) found near the Kumminaghatta village.

5.2 Fuchsite Quartzite

Fuchsite quartzite found near Kummanaghatta village (Fig. 2c) and the sample collected (Fig. 2d) at an old mine operated for fuchsite quartzite appears in greenish color and having a medium grain size which is foliated. Fuchsite, is characteristically present in quartzite observed in the study area, is shown greenish colour which contains significant amount of green fuchsite. The rock is composed almost of quartz and fuchsite. The rock exhibiting bedding plane (S₀) and cleavage relationship, and the strike of N50°W to S50°E dipping 80°W. There are abundant sillimanite, kyanite, staurolite, and chloritoid deposits in the fuchsite quartzites. The quartzite outcrop shows the folded structure in which the right limbs and right limbs are dip in the same direction, is recognized as overturned fold and it has plunge. The part of the limb portion was unfortunately mined-out (Fig.2e).

5.3 Quartzites from Bababudan Group

The Bababudan group is well exposed in the lower part of the Dharwar belt to the east of Ghattihosahalli. Typical oligomict conglomerates are overlain by rhythmic sequences of amygdular metabasalt and cross-bedded quartzites. In general, Bababudan rocks are in sharp contact with Sargur-PGC rock. At various stratigraphic levels of the Bababudan schist belt, quartzites associated with QPC and other quartzites can be found interbedded with volcanic rocks. Quartzites of this type tend to be medium grained, compact, and gray to brown in color. The cross bedded quartzite found near Neralakatte village in the Lower Dharwar of Ghattihosahalli Schist Belt (Fig.2f). The Bababudan Group metasedimentary sequences are found near Neralakatte village, southeast of Talya. Quartzite layers that have recrystallized occur in association with mafic schist. In the samples analyzed, quartz grains predominate with small grains of muscovite (<100 m) & rarely chlorite and there is a minor amount of zircon and/or monazite. It has also been observed that fine crystals of xenotime can be found locally [14].

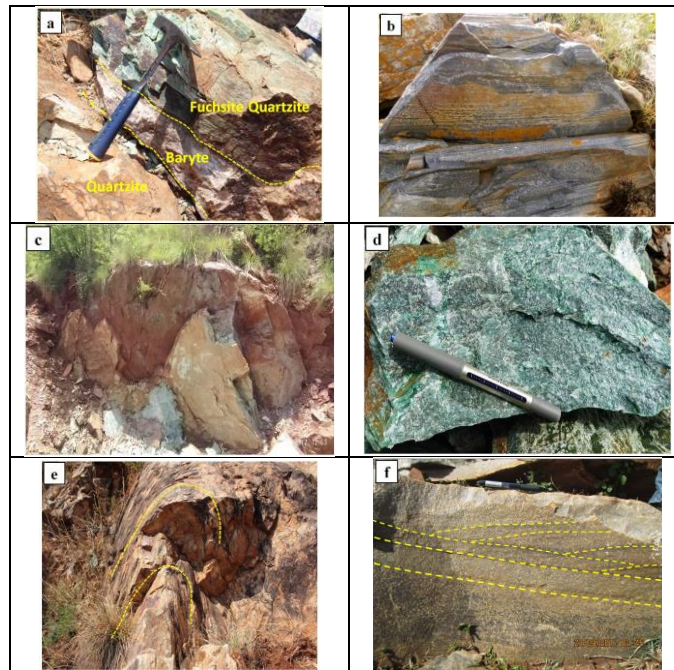


Fig 2: Field photograph of Baryte interbedded with fuchsite quartzite (a) located at a km SSE of Ghattihoshalli village. A Quartzite from old worked quarry pit (b) found near the Kumminaghatta village. Field photograph of Fuchsite quartzite found near Kummanaghatta village (c), the sample of fuchsite quartzite collected (d) from old quarry pit. The quartzite outcrop shows the folded structure (e). The quartzite found near Neralakatte village which exhibit a cross bedded structure (f)

6. PETROGRAPHY

Detailed petrographic and mineralogical features of the quartzites from the study area are presented. About 9 samples of quartzites and 06 fuchsite quartzites were collected from the study area and prepared into thin sections and examined on a polarizing microscope.

6.1 Quartzite

Petrographically, the rock is mainly made up of quartz and minor amount of opaque minerals. Quartzite appears fine to medium grained. In which Quartz occurs as polygonal aggregates, displaying triple junctions (Fig.3a). The edges of these quartz crystals are mostly straight and stepwise. The polygonal quartz aggregates often display subgrains and the larger grains exhibit typical undulose extinction. Some crystals pin the polygonal quartz crystals, while smaller crystals of sericite/muscovite occur as inclusions within these polygonal quartz aggregates (Fig.3b). In Fig.3c a band dominated by muscovite can be observed. Recrystallization of quartz grains is observed while, quartz fragments appears with elongation appearance (Fig.3d). The rock is dominated by quartz, and muscovite with a preference orientation.

6.2 Fuchsite Quartzite

Fuchsite quartzites are essentially made of quartz and Mica (Muscovite), where both the minerals are aligned in such a way gives preferred orientation, in which quartz gains are undergone for recrystallization (Fig. 3e & f). The emerald green color fuchsite mica is pleochroic in nature from yellowish green to green and shows high interference color; while muscovite (Ms) mica shows parallel extinction, are easy to recognize by their clear color in plane-polarized light, with second order interference colors and perfect cleavage.

6.3 Fuchsite-Quartz Schist

The stretched quartz and micas with strong strain shadow is commonly noticed which resembles as preferred orientation. As they have a preferred orientation and they are nearly parallel to each other, they create a lepidoblastic texture (Fig. 3g & h).

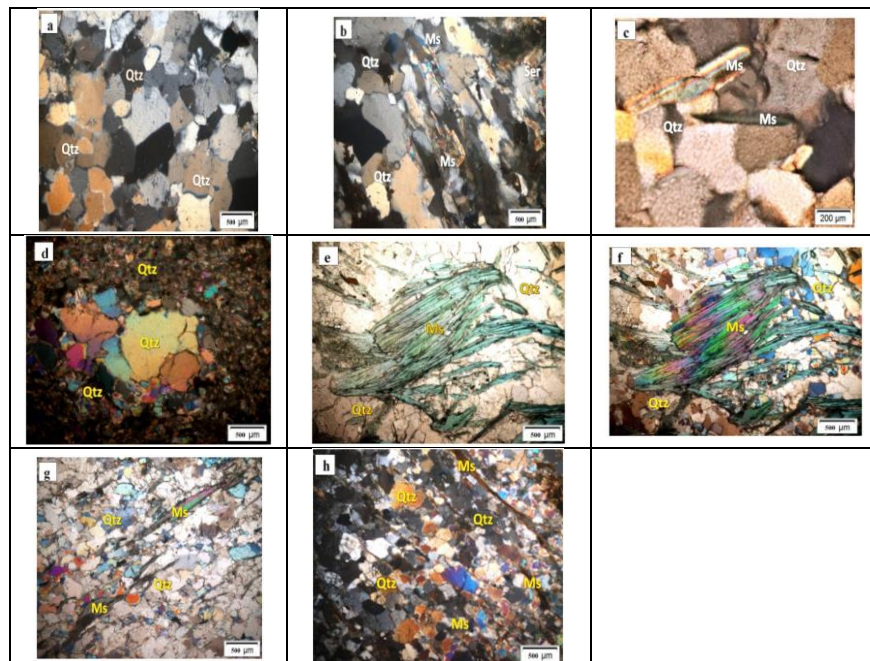


Fig 3: Photomicrographs of Quartzite (a) is exhibiting granoblastic, interlocking and suture texture which consists of quartz as major mineral which occurs as polygonal aggregates, displaying triple junctions. The Muscovite occurs as elongated crystals within quartzite (b). As they have a preferred orientation and there are nearly parallel to each other, they create a lepidoblastic texture & (c) showing granoblastic quartz with wavy extinction and light-green muscovite crystals in a lepidoblastic texture. The recrystallisation is observed (d) while, quartz fragments appears with elongation appearance. The photomicrographs of Fuchsite quartzite observed under plane polarized (e) & under crossed nicol condition (f) which is mainly composed of quartz and the emerald green color fuchsite mica. The anhedral grains of quartz, distinctly bluish green coloured scales and anhedral plates of fuchsite are aligned to produce a planar fabric (g) & (h)

7. RESULTS AND DISCUSSION

7.1 Geochemical Characteristics

It is possible to obtain information about the composition of sedimentary rocks from a geochemical analysis of source rocks, the weathering condition, history of transportation and Conditions of deposit [15], [16]. A lot of research has been conducted on geochemical characteristics in ancient and modern sediment in order to determine the source rocks, provenance, and tectonic setting [1]. Different sedimentary suites have been classified according to their tectonic settings using the major elemental geochemical parameters [17].

7.2 Major Element Geochemistry

The major oxide concentrations data of fuchsite quartzites & quartzites are given in Table 1. The fuchsite quartzites of the study area presents high SiO_2 contents range from 79.69 to 88.9 wt% with an average value of 83.17wt%, Al_2O_3 (8.65-12.1 wt%, average value of 10.18 wt%) while the range and average content of other oxides in the fuchsite quartzites are as follows; TiO_2 (0.15-0.46 wt%, avg 0.31wt %), Fe_2O_3 (0.5-1.89wt%, avg 1.24wt%), MnO (0.001-0.1wt%, avg 0.1wt%), MgO (0.05-0.68wt%, avg 0.47%), CaO (0.05–0.83 wt%, avg 0.33wt%), Na_2O (0.24–0.66 wt%, avg 0.51wt%), K_2O (1.15-5.21wt%, avg 3.21 wt%) and P_2O_5 contents (0.02-0.57 wt%, avg 0.25wt%). The quartzite shows higher value of SiO_2 (88.34-96.14wt%, avg 92.68wt%), Al_2O_3 (2.18-6.80 wt%, avg 3.90 wt%) depleted in TiO_2 (0.04-0.60 wt%, avg 0.21wt %), Fe_2O_3 (0.09-0.51wt%, avg 0.31wt%), MnO (0.01-0.02wt%, avg 0.01wt%), MgO (0.05-0.26wt%, avg 0.10%), CaO (0.04-0.37 wt%, avg 0.13wt%), Na_2O (0.20-0.37 wt%, avg 0.28wt%), K_2O (0.28-2.15wt%, avg 1.04 wt%) and P_2O_5 contents (0.01-0.26 wt%, avg 0.06wt%) contents.

Table 1: Major Oxides (wt%) concentrations of fuchsite quartzites & quartzites from the Ghattihosahalli Schist Belt area

Sample No	Fuchsite Quartzites						Quartzites								
	GH-24	GH-29	KG-159	GH-34	KG-87	GH-160	NK-91	KG-73	NK-95	GH-61	NK-161	NK-162	NK-158	KG-18	KG-17
SiO ₂	88.90	79.96	83.24	82.65	79.69	84.57	95.89	89.79	96.01	92.69	95.87	88.34	96.14	89.78	89.59
TiO ₂	0.20	0.32	0.46	0.37	0.38	0.15	0.06	0.05	0.06	0.04	0.09	0.58	0.12	0.34	0.60
Al ₂ O ₃	8.65	9.81	12.1	11.5	9.89	9.15	2.18	2.98	2.66	2.87	2.23	6.7	2.19	6.53	6.80
Fe ₂ O ₃	0.00	1.89	1.63	0.5	1.85	1.56	0.33	0.39	0.47	0.35	0.21	0.09	0.32	0.51	0.10
MnO	0.01	0.001	0.01	0.01	0.001	0.01	0.00	0.01	0.01	0.01	0.00	0.01	0.00	0.02	0.02
MgO	0.05	0.63	0.48	0.05	0.68	0.57	0.08	0.11	0.07	0.11	0.1	0.05	0.08	0.26	0.06
CaO	0.05	0.43	0.17	0.06	0.41	0.83	0.04	0.09	0.04	0.14	0.05	0.3	0.06	0.04	0.37
Na ₂ O	0.66	0.57	0.61	0.36	0.24	0.63	0.26	0.37	0.25	0.31	0.2	0.52	0.21	0.20	0.24
K ₂ O	1.36	5.21	1.15	4.92	5.11	1.49	0.60	1.65	0.61	0.28	0.59	1.98	0.63	0.89	2.15
P ₂ O ₅	0.00	0.57	0.3	0.04	0.59	0.02	0.01	0.04	0.01	0.04	0.03	0.02	0.03	0.06	0.26
Total	99.88	99.39	100.15	100.46	98.84	98.98	99.45	95.48	100.19	96.84	99.37	98.59	99.78	98.45	100.19
K ₂ O/Na ₂ O	2.06	9.14	1.89	13.67	21.29	2.37	2.31	4.46	2.44	0.90	2.95	3.81	3.00	4.45	8.96
K ₂ O+Na ₂ O	2.02	5.78	1.76	5.28	5.35	2.12	0.86	2.02	0.86	0.59	0.79	2.50	0.84	1.09	2.39
K ₂ O/Al ₂ O ₃	0.16	0.53	0.10	0.43	0.52	0.16	0.28	0.55	0.23	0.10	0.26	0.30	0.29	0.14	0.32
Fe ₂ O ₃ /MgO	0.00	3.00	3.40	10.00	2.72	2.74	4.13	3.55	6.71	3.18	2.10	1.80	4.00	1.96	1.67
Fe ₂ O ₃ +MgO	0.05	2.52	2.11	0.55	2.53	2.13	0.41	0.50	0.54	0.46	0.31	0.14	0.40	0.77	0.16
Al ₂ O ₃ /TiO ₂	43.25	30.66	26.30	31.08	26.03	61.00	36.33	59.60	44.33	71.75	24.78	11.55	18.25	19.21	11.33
SiO ₂ /Al ₂ O ₃	10.28	8.15	6.88	7.19	8.06	9.24	43.99	30.13	36.09	32.30	42.99	13.19	43.90	13.75	13.18
Log(SiO ₂ /Al ₂ O ₃)	1.01	0.91	0.84	0.86	0.91	0.97	1.64	1.48	1.56	1.51	1.63	1.12	1.64	1.14	1.12
Log(Na ₂ O/K ₂ O)	-0.31	-0.96	-0.28	-1.14	-1.33	-0.37	-0.36	-0.65	-0.39	0.04	-0.47	-0.58	-0.48	-0.65	-0.95
Log(Fe ₂ O ₃ /K ₂ O)	0.00	-0.44	0.15	-0.99	-0.44	0.02	-0.26	-0.63	-0.11	0.10	-0.45	-1.34	-0.29	-0.24	-1.33
CIA	76.56	62.07	86.81	65.98	61.01	69.00	65.94	54.75	70.36	74.70	63.23	65.71	61.47	80.11	68.57
PIA	85.92	92.16	94.81	91.07	84.66	75.11	76.26	63.83	81.30	79.33	82.05	77.11	79.76	95.57	90.95
CIW	88.03	96.51	95.32	95.00	92.61	78.56	82.06	81.50	85.26	81.10	86.50	83.20	85.12	96.20	93.86

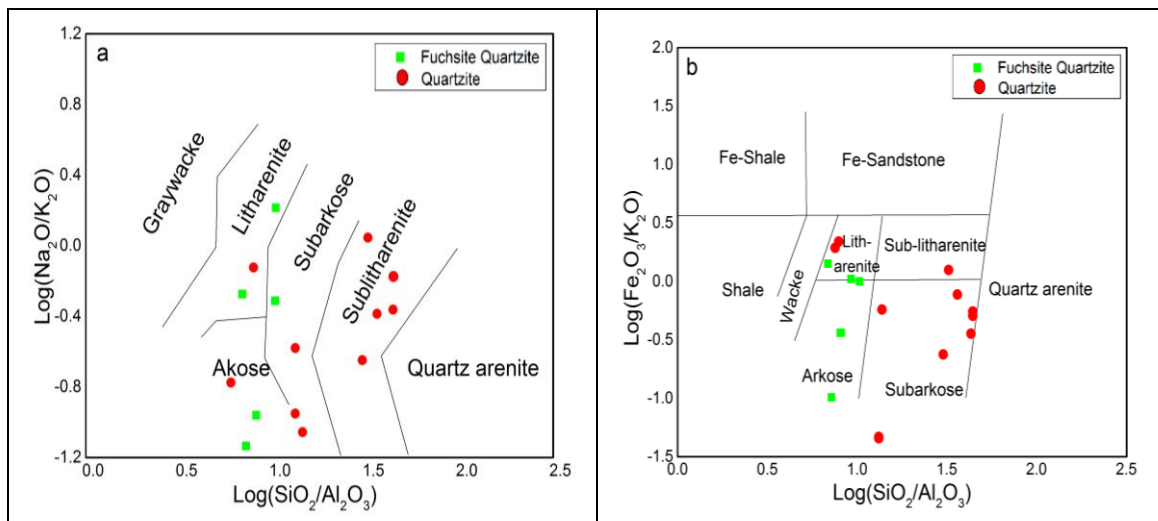
The major oxides have been used by a number of researchers in order to classify terrigenous sediments geochemically. Mineral stability is measured by the ratio of the $\text{SiO}_2/\text{Al}_2\text{O}_3$ ratio and the $\text{Na}_2\text{O}/\text{K}_2\text{O}$ ratio, although the $\text{Fe}_2\text{O}_3/\text{K}_2\text{O}$ ratio gives a more accurate indication of mineral stability [18].

The fuchsite quartzite samples plotted in $\log (\text{SiO}_2/\text{Al}_2\text{O}_3)$ vs $\log (\text{Na}_2\text{O}/\text{K}_2\text{O})$ represent arkose to litharenite, while quartzites plotted in the subarkose to sublitharenite field (Fig. 4a).

In addition, Binary plot by Heron [19] of $\log (\text{SiO}_2/\text{Al}_2\text{O}_3)$ vs. $\log (\text{Fe}_2\text{O}_3/\text{K}_2\text{O})$, Fuchsite quartzite samples occupy the field arkose and litharenite and whereas the quartzite samples occupies the field of subarkose, and few in litharenite and sublitharenite field (Fig. 4b). It is clear from the Na_2O vs. K_2O plot diagram by Crook [20], that the majority of the samples studied are located in quartz rich field (Fig. 4c). Based on the $\text{K}_2\text{O}/\text{Al}_2\text{O}_3$ values, sedimental primary composition can be determined [21].

$\text{K}_2\text{O}/\text{Al}_2\text{O}_3$ values, for example, range from (0.3–0.9) in feldspars and (0.0–0.3) in clay minerals. According to the present study, the $\text{K}_2\text{O}/\text{Al}_2\text{O}_3$ values of quartzites range from 0.10 to 0.55 (average 0.34), indicating that K-feldspars and micas are more abundant than clay minerals in the provenance.

It is consistent with the petrographic interpretations of the studied quartzites that $\text{K}_2\text{O}/\text{Na}_2\text{O}$ ratios are greater than one, indicating a dominance of feldspar over plagioclase.



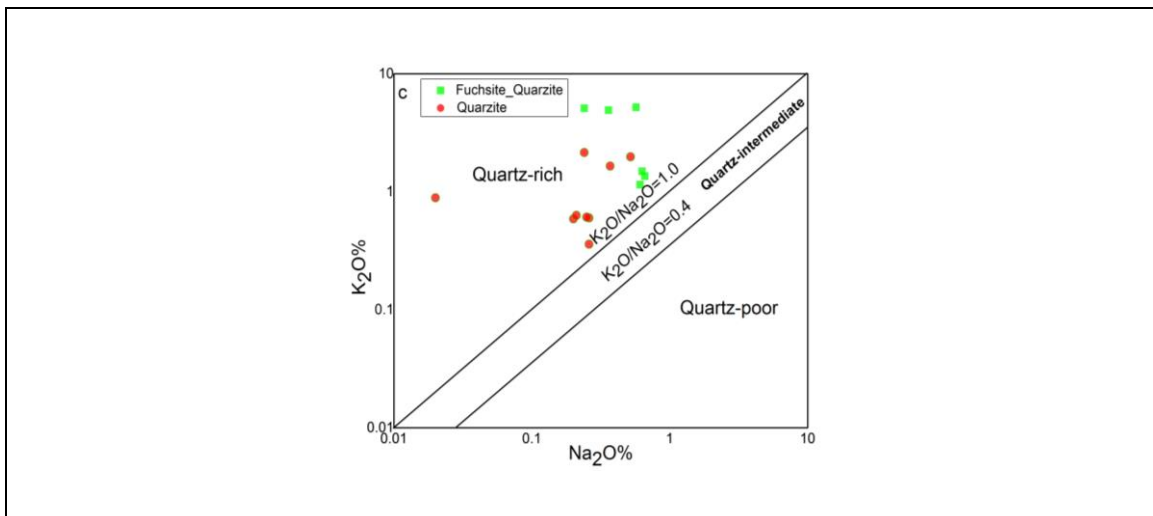


Fig 4: Chemical classification diagrams of fuchsite quartzite & quartzite discriminating according to logarithmic ratio of $\text{SiO}_2/\text{Al}_2\text{O}_3$ vs. $\text{Na}_2\text{O}/\text{K}_2\text{O}$ (Fig a: Fields after Pettijohn et al., [18]), $\text{Fe}_2\text{O}_3/\text{K}_2\text{O}$ (Fig b: Fields after Herron, [19]) and Na_2O vs. K_2O diagram (Fig c: Fields after Crook., [20])

7.3 Trace Element Geochemistry

Trace elements have distinct signatures that are primarily influenced by the minerals in which they are contained. A majority of trace elements in clastic rocks can be found in clay minerals, according to several researchers [3].

The presence of trace elements in sediments is generally well retained during weathering and transportation. Consequently, analyzing the composition and content of trace elements in sediments can be helpful in identifying a source rock's characteristics and structural features [1], [16].

The trace element concentration data for fuchsite quartzites & quartzites are given in Table 2.

The range and average value of selected trace elements in the studied samples are as follows: For Fuchsite quartzites, Th (1.00 ppm), Ni (1ppm), Sr (58 - 75ppm, 68.33), Ba (7980 - 8937 ppm, 8469.33), Rb (35 -48 ppm,41.16), Y (5 - 7 ppm, 5.66), Zr (11 - 15ppm,12.5), Pb (6 - 11ppm,9), Zn(95 -110 ppm,104.16), V (98 - 110 ppm,104.33) and Cr (570 -993ppm, 825.5) and where as for quartzites, Th (2-5.1ppm, 3.0), Ni (0.81-2.21ppm, 1.55), Sr (7 -11.12ppm, 9.95), Ba (35 - 79ppm, 69.44), Rb (14 - 44ppm,19.65), Y (2.85 - 15 ppm, 5.57), Zr (39 - 192ppm,68), Pb (1- 4ppm,2.62), Zn (4 -12 ppm, 8.7), V (3 - 18 ppm,7.92) and Cr (28 -118ppm,54).

Table 2: Geochemical data of trace elemental distribution in Quartzites from the study area

Sample No	Fuchsite Quartzites						Quartzites								
	GH-24	GH-29	KG-159	GH-34	KG-87	GH-160	NK-91	KG-73	NK-95	GH-61	NK-161	NK-162	NK-158	KG-18	KG-17
Ba	8937	8687	7980	8121	8681	8410	74	79	74	72	78	35	69	76	68
Rb	46	37	42	48	39	35	16	13.09	15.78	14	18	44	17	18	21
Sr	69	71	58	66	71	75	8	9.47	11	9	7	15	8	11	11.12
Y	6	5	7	6	5	5	4	3.98	2.85	3.33	3.43	15	4.55	7	6
Zr	13	12	13	11	11	15	56	39	45	53	59	64	49	60	59
Nb	*	*	*	*	*	*	1	1.69	2.31	1.11	1.51	4	1.1	1.7	1.66
Th	1	1	1	1	1	1	2	4.02	2.68	2.7	5.1	2.6	2.97	3	2
Pb	10	8	11	10	9	6	3	2	3	3	3	*	1	4	2
Ga	7	7	6	7	7	6	2	0.61	1.82	1.5	2	1.2	6.76	3	2.89
Zn	108	110	106	98	108	95	12	11	11.4	11.1	4	1.21	8.7	9	10
Cu	5	5	6	4	5	5	3	4	3	3	5	3.8	2.65	4	3
Ni	1	1	1	1	1	1	1	0.76	1.2	0.81	2	1.9	2.21	2	2.13
V	103	110	102	104	109	98	6	4.44	5.2	5.7	3	18	16	7	6
Cr	993	797	912	874	807	570	28	37	42	31	85	118	83	33	29
Sc	2	2	1	3	2	1	2	1.66	2.5	2	2.57	2.9	2.3	1	2.62
Co	*	*	*	*	*	*	*	*	*	*	*	*	*	*	*
U	*	*	*	*	*	*	*	*	*	*	*	*	*	*	*
Co+Cr+Sc	995	799	913	877	809	571	30	39	45	33	88	121	85	34	32

(*) BDL: BELOW DETECTION LIMIT

Due to the higher proportion of potash feldspar in rocks of provenance, the studied samples have high Rb contents. A low Rb/Sr ratio indicates that feldspar has been altered and weathered either at the source or during transportation. It has been determined that the Cr content of Fuchsite quartzites (570-993ppm) is higher than that of UCC and PAAS, while the Cr content of quartzites (28-118ppm) is lower than that of UCC and PAAS. Because of the presence of fuchsite in quartzite, the high concentration of Cr occurs. Additionally, since these rocks are structurally overlain by bedded barytes and Ba-rich fuchsite quartzite, the high Ba content can be observed in the form of barium feldspar (celsian) and barite grains [22]. Normalized multi-element spider diagrams for trace elements in upper continental crust (UCC) quartzites (Fig.5.a) show slight enhancement of Cr and reduction of Rb, Ba, Th, Nb, Sr; on the other hand, Fuchsite quartzites (Fig.5.b) exhibit slight improvement of Ba, Cr, V, and reduction of Sr, Th, and Rb.

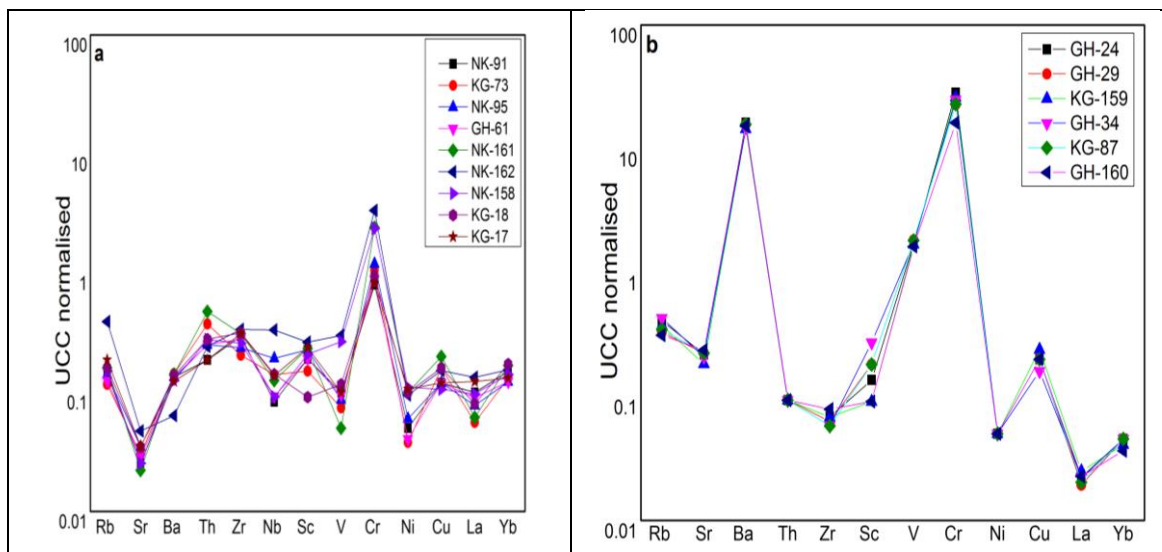


Fig 5: Upper continental crust trace element normalized plot for the studied (a) quartzites and (b) Fuchsite Quartzite (UCC values after McLennan [39])

A shallow marine basin underlain by spinifex-textured komatiitic and basaltic volcanic rocks deposited pelitic and semipelitic strata in the GHSB. Based on the preservation of detrital chromite within Cr-bearing accessory minerals, it is suggested that it was deposited in a granitoid-greenstone terrain with the clastic detritus [23]. During diagenetic stages, the Ba content of white mica and sporadic barian K-feldspar may have increased due to interactions with intra-formational Ba, Cr-bearing fluids rising from komatiitic and basaltic sub-seafloors [24].

7.4 Rare Earth Element Geochemistry

There is a general perception that rare earth elements (REEs) are immobile, as they exhibit only minor changes as a result of sedimentation processes. Primary factors responsible for controlling their presence in sediments are the abundance of these elements in source rocks and weathering conditions in the provenance region. Both syn-depositional and post-depositional processes are insignificant in altering the REE content of sediments during transportation, deposition, and diagenesis [25], [26]. Research has demonstrated that the relationship between provenance type, source rocks, and the composition of sandstone is governed by plate tectonics [20], [27], [28], [29], [30].

The range and average concentration of selected rare earth elements in Fuchsite quartzite is as follows: La (0.56 -0.75ppm, 0.65), Ce (0.69 -0.89ppm, 0.79), Nd (0.42 - 0.61 ppm, 0.51), Sm (0.28 - 0.34 ppm, 0.31), Eu (0.05 -0.08 ppm, 0.06), Gd (0.24- 0.31ppm, 0.27) and Yb (0.08 – 0.1ppm, 0.09), Σ REEs 3.00 -3.42 ppm, average 3.16 ppm; and for quartzite La (1.68 -4ppm, 2.72), Ce (3.41 -6ppm, 4.74), Nd (1.11 – 2.8 ppm, 1.64), Sm (0.23-0.45 ppm, 0.33), Eu (0.08-0.14ppm, 0.10), Gd (0.23 – 0.58ppm, 0.37) and Yb (0.27 – 0.38ppm, 0.31). Σ REEs 9.13 -15.68 ppm, average 11.72 ppm. The REE data is presented in the Table 3.

Table 3: Geochemical data showing Rare Earth elements in Quartzites from the study area

Sample No	Fuchsite Quartzites						Quartzites								
	GH-24	GH-29	KG-159	GH-34	KG-87	GH-160	NK-91	KG-73	NK-95	GH-61	NK-161	NK-162	NK-158	KG-18	KG-17
La	0.66	0.58	0.75	0.67	0.61	0.68	3.00	1.68	2.33	2.7	1.85	4	2.9	2.4	3.7
Ce	0.83	0.71	0.89	0.81	0.73	0.82	4.35	3.8	5.72	3.41	4.1	6	5.1	5.23	5
Pr	0.15	0.13	0.11	0.15	0.14	0.16	0.5	0.43	0.63	0.47	0.51	0.6	0.4	1	0.48
Nd	0.39	0.49	0.32	0.37	0.48	0.36	1.51	1.51	1.89	1.49	1.49	2.8	1.62	1.42	1.11
Sm	0.67	0.58	0.61	0.59	0.63	0.68	0.32	0.23	0.28	0.29	0.36	0.38	0.33	0.45	0.22
Eu	0.12	0.13	0.12	0.13	0.14	0.11	0.1	0.04	0.08	0.04	0.13	0.19	0.11	0.18	0.14
Gd	0.32	0.36	0.33	0.3	0.38	0.29	0.39	0.34	0.21	0.27	0.33	0.4	0.37	0.56	0.42
Tb	0.01	0.02	0.01	0.01	0.02	0.01	0.06	0.03	0.05	0.06	0.07	0.05	0.05	0.05	0.04
Dy	0.06	0.05	0.05	0.06	0.05	0.05	0.42	0.41	0.35	0.29	0.42	0.51	0.44	0.47	0.39
Ho	0.02	0.02	0.02	0.02	0.02	0.02	0.09	0.07	0.05	0.07	0.08	0.08	0.09	0.1	0.08
Er	0.05	0.04	0.04	0.04	0.05	0.05	0.29	0.21	0.32	0.28	0.27	0.3	0.3	0.35	0.28
Tm	0.01	0.01	0.01	0.01	0.01	0.01	0.04	0.02	0.04	0.04	0.05	0.05	0.04	0.03	0.02
Yb	0.1	0.1	0.09	0.1	0.1	0.08	0.33	0.29	0.27	0.27	0.37	0.34	0.31	0.38	0.29
Lu	0.11	0.13	0.12	0.11	0.11	0.12	0.05	0.03	0.03	0.04	0.05	0.04	0.06	0.04	0.03
ΣREE	3.5	3.35	3.47	3.37	3.47	3.44	11.45	9.09	12.25	9.72	10.08	15.74	12.12	12.66	12.2
ΣLREE	3.14	2.98	3.13	3.02	3.11	3.1	10.17	8.03	11.14	8.67	6.25	14.37	10.83	11.24	11.07
ΣHREE	0.36	0.37	0.34	0.35	0.36	0.34	1.28	1.06	1.11	1.05	1.31	1.37	1.29	1.42	1.13
ΣLREE/ΣHREE	8.72	8.05	9.21	8.63	8.64	9.12	7.95	7.58	10.04	8.26	4.77	10.49	8.40	7.92	9.80
Average	0.25	0.24	0.25	0.24	0.25	0.25	0.82	0.65	0.88	0.69	0.72	1.12	0.87	0.90	0.87
Eu/Eu*	0.79	0.87	0.82	0.94	0.87	0.76	0.87	0.44	1.01	0.44	1.15	1.49	0.96	1.10	1.41
(La/Sm)N	0.62	0.63	0.77	0.71	0.61	0.63	5.90	4.60	5.24	5.86	3.23	6.63	5.53	3.36	10.59
(La/Yb)N	4.46	3.92	5.63	4.53	4.12	5.74	6.14	3.91	5.83	6.76	3.38	7.95	6.32	4.27	8.62
(Gd/Yb)N	2.59	2.92	2.97	2.43	3.08	2.94	0.96	0.95	0.63	0.81	0.72	0.95	0.97	1.19	1.17

The Chondrite normalized REE are fractionated in fuchsite quartzites and quartzites with low HREE (Fig.6a & 6b). (La/Sm) N values having range of 1.07-1.53 in fuchsite quartzite and 3.23 - 6.85 in quartzite. (Gd/Yb) N values range between 1.95-2.94 in fuchsite quartzite and 0.69-1.24 in quartzite, which are related to LREE enrichment in the fuchsite quartzite and quartzite. The fractionated REE value of (La/Yb) N varies between 3.92 and 6.17 in fuchsite quartzite, and 3.38 to 8.62 in quartzite. Fuchsite quartzite and quartzite exhibit a Eu anomaly between 0.57 and 0.83 and 0.75 to 1.31, which may be caused by the presence of felsic igneous rocks depleted in Eu, such as granite, in the provenance. An enrichment of LREE has been observed in quartzites with almost fractionated HREE, which is likely related to the presence of monazite, zircon, and xenotime grains observed in the petrographic analysis. The relative fractionation of REE in Archean quartzite combined with a depleted HREE indicates that mafic and ultramafic rocks were present at the source.

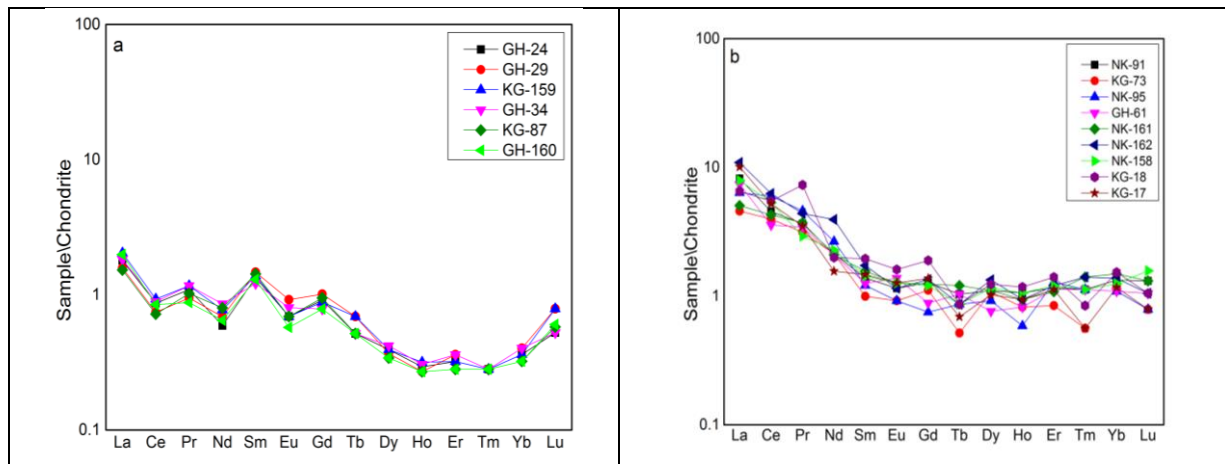


Fig 6: Chondrite normalized (Taylor and McLennan [3]) rare earth element (REE) pattern for the studied (a) Fuchsite quartzites & (b) quartzites

8. PALEO-WEATHERING

Chemical weathering is influenced by climate and tectonic uplift, which determine its rate/intensity and extent. A-CN-K ternary plots and chemical indices of alteration (CIA) can be used to determine the weathering and diagenesis of sedimentary rocks, as well as the climatic conditions at the time of formation [6], [31]. [42], The chemical index of alteration is used to determine the extent of chemical alteration of the provenance by using the equation: $CIA = [Al_2O_3 / (Al_2O_3 + CaO^* + Na_2O + K_2O)] \times 100$ in molecular proportions, CaO^* symbolize the Ca of silicate fraction. The range and average of chemical weathering index values for the studied samples (Fuchsite quartzites 61.01 - 86.81, avg.70.24; Quartzites 54.75 - 86.39, avg. 67.90) indicate general chemical weathering to be moderate to moderately intense. The samples were plotted onto a triangular diagram of Al_2O_3 - CaO^* - Na_2O - K_2O (A-CN-K) (Fig.7a) to determine the provenance and weathering trends. As a result of the study, most samples fall near the corner of Al_2O_3 , indicating that chemical weathering is moderate to high. As shown in the diagram, Fuchsite Quartzite and Quartzite samples plotted along the A-K line nearby the muscovite-illite region, which illustrate that weathering trend of granite, granodiorite, and tonalite along the plagioclase -K-feldspar line. An analysis of the trend lines and points on the A-CN-K diagram reveals the origin of the sedimentary suites. It has been found that the majority of the samples studied have a granite source and few samples that fall between granodiorite and tonalite sources. The chemical index of weathering (CIW) is calculated using the equation $CIW = [Al_2O_3 / (Al_2O_3 + CaO^* + Na_2O)] \times 100$. The samples of Fuchsite quartzites exhibit values range from 78.56 to 96.51 (average 91) and quartzites exhibit values range from 81.10 to 99 (average 86.40), further indicating moderate to severe weathering conditions were experienced by the source terrain of the studied samples. Chemical weathering can also be determined by using PIA [6] in molecular proportions, which can be calculated by the equation, $PIA = (Al_2O_3 - K_2O) / (Al_2O_3 + CaO^* + Na_2O - K_2O) \times 100$. Fuchsite quartzite has a PIA range of 75.11 to 92.16 (average 87.29),

whereas quartzites have a PIA range of 63.83 to 98.83 (average 81.05), indicating a high proportion of plagioclase alteration. According to the AK-C-N ternary diagram (Fig.7b), Quartzite and Fuchsite quartzites belong to the oligoclase and albite fields. Based on the results, it appears that plagioclase has been altered nearly completely in the majority of samples. According to the CIA and PIA of the samples in study area, there is a moderate level of chemical alteration and a high level of PIA for these samples. Based on the CIA, PIA, CIW and A-CN-K diagrams, it appears the studied samples have undergone moderate to high chemical weathering. Based on the bivariate plot of SiO_2 vs. $\text{Al}_2\text{O}_3 + \text{K}_2\text{O} + \text{Na}_2\text{O}$ proposed by Suttner and Dutta [32], the climatic conditions for quartzite formation were identified (Fig. 7c). It is evident from the plot that the studied quartzite samples are from a source that has been exposed to semi humid climate environment, whereas the fuchsite quartzite samples originate from a source that has experienced semiarid to semi humid climate environment.

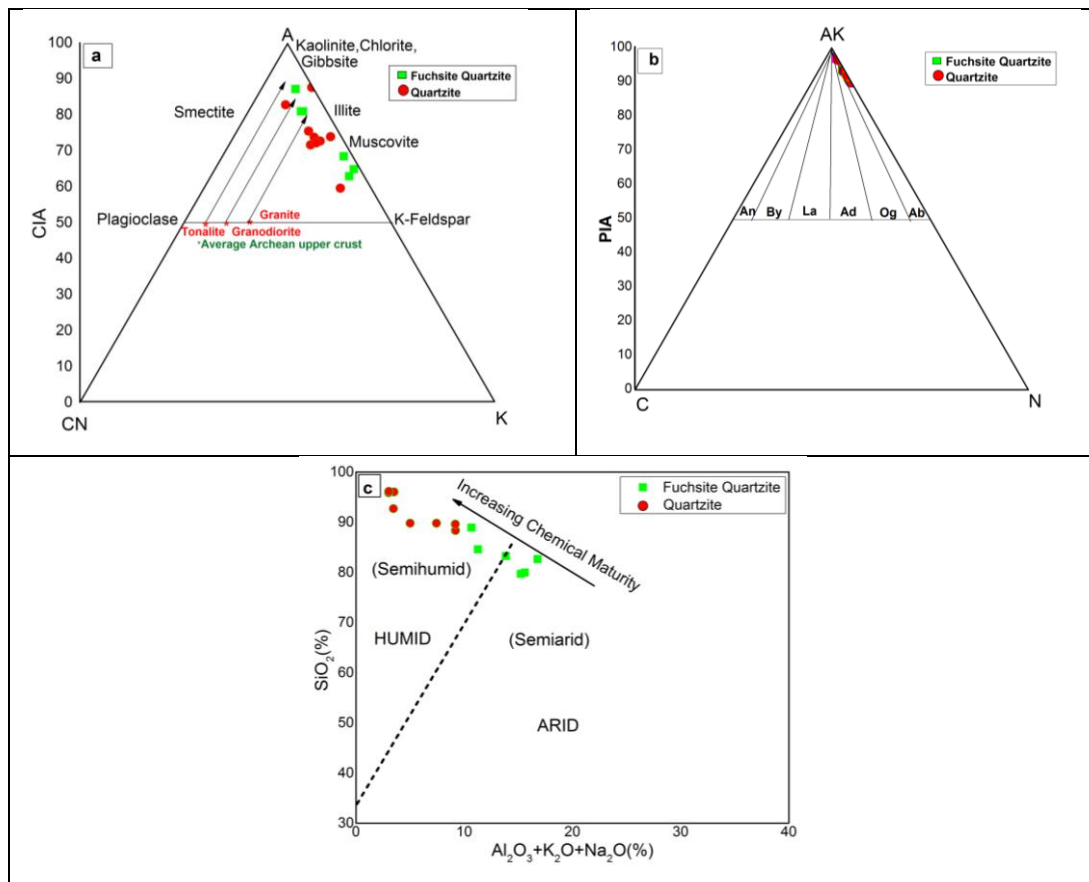


Fig 7: (a) A-CN-K ($\text{Al}_2\text{O}_3\text{-CaO}^* + \text{Na}_2\text{O-K}_2\text{O}$) ternary diagram (Nesbitt & Young [42]) and the arrow shows the trend of weathering and alteration (Condie [40]) was used in which majority of the quartzite samples cluster along the A-K line. (b) The quartzites samples occupy the fields of alkali feldspar in the AK-C-N ternary diagram (Fedo et al., [6]). (c) Chemical maturity of the fuchsite quartzites and quartzites of the study area was depicted from the bivariate plot of SiO_2 vs. $\text{Al}_2\text{O}_3 + \text{K}_2\text{O} + \text{Na}_2\text{O}$ (Field after Suttner & Dutta, [32])

9. PROVENANCE

In the context of determining provenance, geochemistry provides important information, particularly for fine-grained sedimentary rocks [16]. The values plotted on discrimination function diagram after Roser and Korsch [2] which shows that the studied samples are part of the quartzose sedimentary field (Fig.8a). As shown in the diagram of Zr versus TiO₂ used by Hayashi et al [33], Fig.8b, the analyzed samples belong to the felsic and mafic zones. It has been reported by Hayashi et al [33] that the Al₂O₃/TiO₂ ratio for mafic igneous rocks varies from 3 to 8, for intermediate igneous rocks varies from 8 to 21, and for felsic igneous rocks varies from 21 to 70. For the studied samples, Al₂O₃/TiO₂ value ranges from 11.33–71.75. Thus, the high values of Al₂O₃/TiO₂ ratio indicative of felsic igneous rocks are the source of these samples. In the equation of Hayashi et al [33] SiO₂ (%) = 39.34 + 1.2578*(Al₂O₃/TiO₂) - 0.0109*(Al₂O₃/TiO₂)², the Al₂O₃/TiO₂ values of quartzites are calculated. As a result of the equation, computed SiO₂ contents ranging from 52.20 to 73.47 wt%, with an average of 66.26wt% and is attributed to felsic igneous rocks as the source of the studied samples.

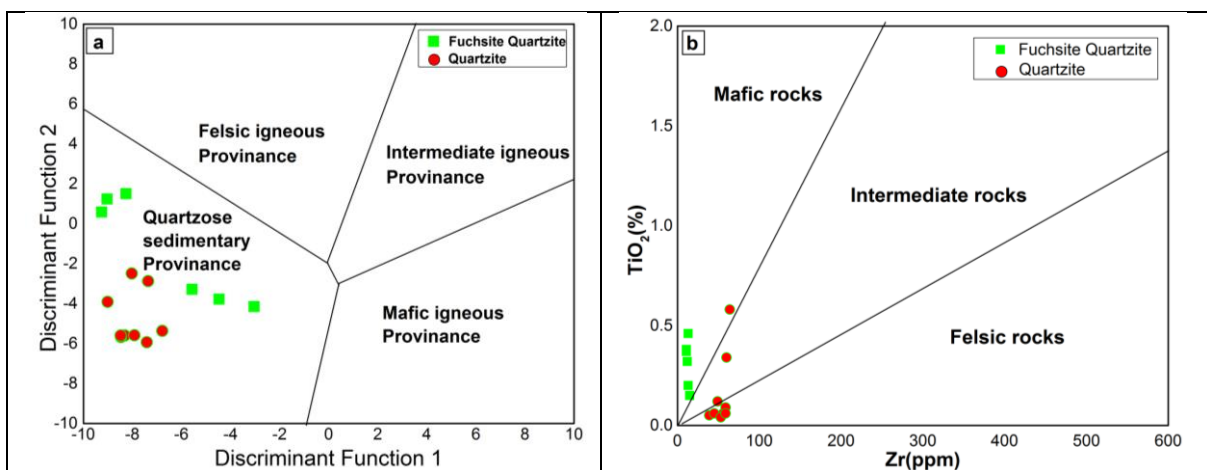


Fig 8: (a) Possible provenance for quartzites and fuchsile quartzites, are depicting through discriminant function, DF-1 vs. DF-2 plot (Roser & Korsch [2])
 $DF1 = (-1.773 \times TiO_2) + (0.607 \times Al_2O_3) + (0.76 \times Fe_2O_3) - (1.5 \times MgO) + (0.616 \times CaO) + (0.509 \times Na_2O) - (1.224 \times K_2O) - 9.09$; $DF2 = (0.445 \times TiO_2) + (0.07 \times Al_2O_3) - (0.25 \times Fe_2O_3) - (1.142 \times MgO) + (0.438 \times CaO) + (1.475 \times Na_2O) + (1.426 \times K_2O) - 6.861$. (b) TiO₂-Zr plot (Hayashi et al., [33]) for the studied quartzites

It is evident from the TiO₂/Ni ratio (Fig. 9a) that the studied quartzites are of felsic origin [34]. In the Th/Sc vs. Sc plot, studied quartzites are likely to occur in the vicinity of sandstone and granite, as well as away from basalt, andesite, and komatiite (Fig. 9b).

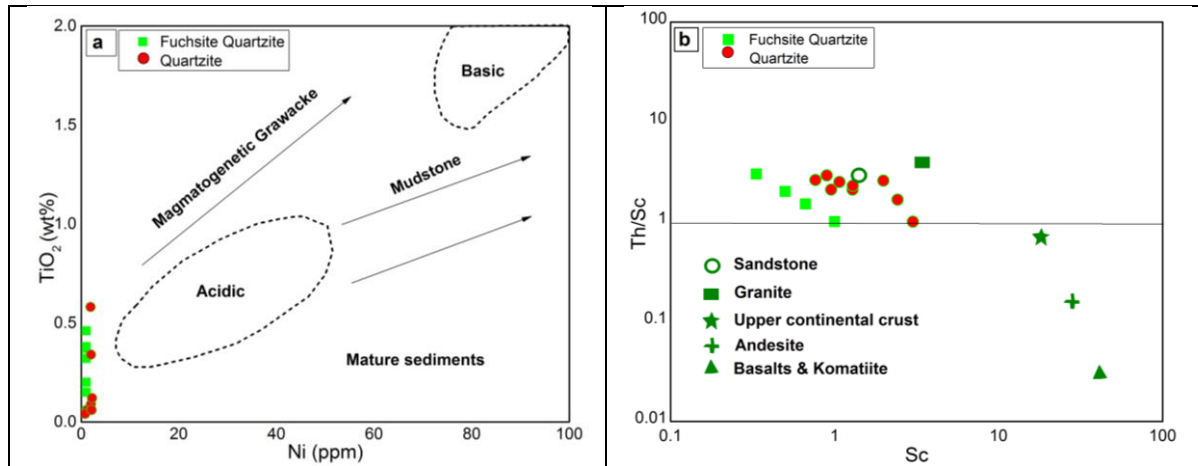


Fig 9: (a) TiO₂ vs. Ni diagram is selected for identifying the provenance for studied quartzites (Floyd et al., [34]); (b) Th/Sc vs. Sc binary plot of quartzites falling within the sandstone (Values of UCC from McLennan [39] and sandstone, andesite, basalt and komatiite fields are from Condie [40])

As determined by the ratios Eu/Eu*, La/Sc, Th/Sc, and Cr/Th of fuchsite quartzite, it has average values of 0.66, 0.45, 0.67, and 825.50, while quartzite has average values of 0.93, 1.31, 1.52, and 18.43 respectively. Thus which is also implies that studied samples are likely to be derived from felsic and mafic rock sources (Table 4).

Table 4: Range of elemental ratios of Fuchsite quartzite & quartzite compared with the ratios derived from felsic rocks, mafic rocks and upper continental crust

Elemental ratio	Fuchsite quartzite	Quartzite	Ranges in sediments from felsic sources ^(a)	Ranges in sediments from mafic sources ^(a)	Upper continental crust ^(b)
Eu/Eu*	0.57-0.83 (~0.66)	0.75-1.31 (~0.93)	0.40-0.94	0.71-0.95	0.63
La/Sc	0.22-0.75 (~0.45)	0.93-2.40 (~1.31)	2.50-16.3	0.43-0.86	2.21
Th/Sc	0.33-1.0 (~0.67)	0.76-3.0 (~1.52)	0.84-20.5	0.05-0.22	0.79
La/Co	-	-	1.80-13.8	0.14-0.38	1.76
Th/Co	-	-	0.67-19.4	0.04-1.40	0.63
Cr/Th	570-993 (~825.50)	9.20-45.38 (~18.43)	4.00-15.0	25-500	7.76

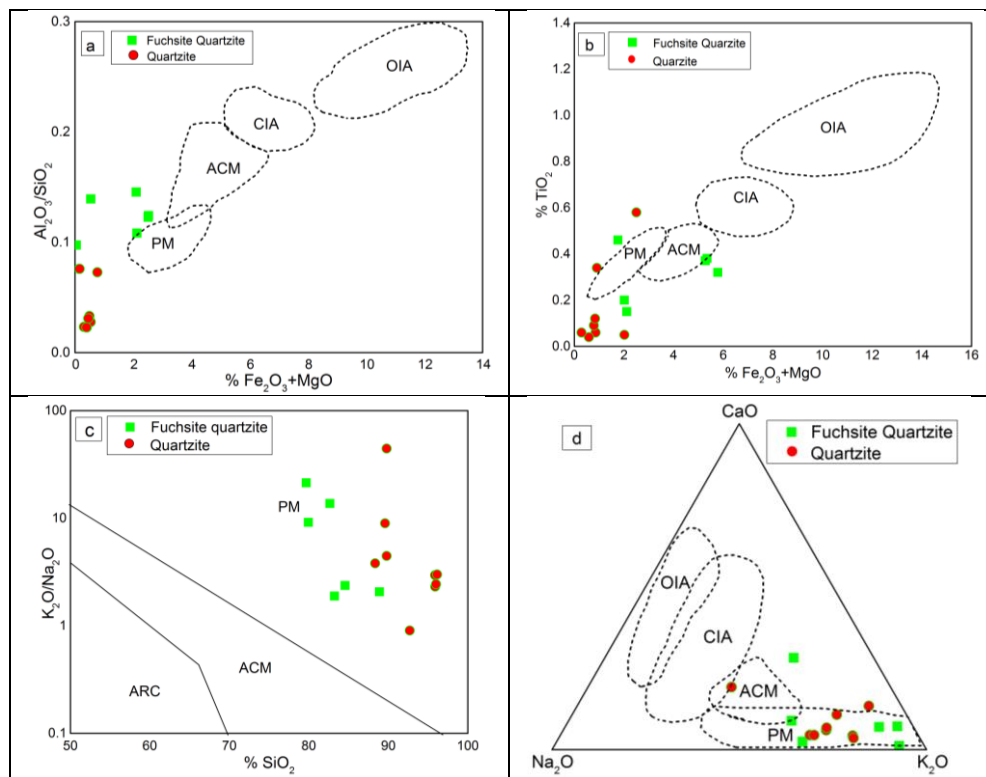
^(a)Cullers et al [43]; Cullers [44]; Cullers and Podkovyrov [45]; ^(b)McLennan [39]; Taylor and McLennan[3].

Devaraju and Ananthamurthy [35] concluded that the essential elements required for the formation of fuchsite either existed within the sediment itself, possibly within the hydrolyzed/shaly matter of the sandstone, or were partially or completely supplied to the rock through volcanic exhalation that is believed to have been a key factor in the formation of the close related barite beds. Chromiferous quartzites in the Sargur Group are largely

metamorphosed sediments deriving from silica, with ultramafic rocks enclaved within them.

10. TECTONIC SETTING

Geochemical characteristics of sediments are closely related to the provenance of the sediments as well as the tectonic environment in which they were formed. Several parameters have been extensively studied in order to interpret the tectonic setting of sediments and sedimentary rocks, including major oxides, traces, and REE. The composition of major elements has been used to discriminate sedimentary basins based on their tectonic setting [17], [36]. An illustration of the tectonic setting of quartzite can be obtained using common discrimination diagrams, such as Al_2O_3/SiO_2 vs. $Fe_2O_3 + MgO$ and TiO_2 vs. $Fe_2O_3 + MgO$ after Bhatia [17]. It is evident from the diagram of Al_2O_3/SiO_2 versus Fe_2O_3+MgO that all of the samples are located near the passive margin (Fig. 10a), whereas in TiO_2 vs. Fe_2O_3+MgO plot, most of the samples are located in the vicinity of the passive margin and few are located near the active continental margin field (Fig. 10b). On the basis of Roser and Korsch's [36] plot of SiO_2 vs. K_2O/Na_2O , all quartzites are located in passive margin settings (Fig. 10c). In the ternary diagram of $CaO-N_2O-K_2O$ after Bhatia, [17] (Fig.10d) & in the $SiO_2/20-K_2O+Na_2O-TiO_2+Fe_2O_3+MgO$ diagram after Kroonenberg [37] (Fig.10e), the majority of quartzite samples are plotted in the passive margin setting.



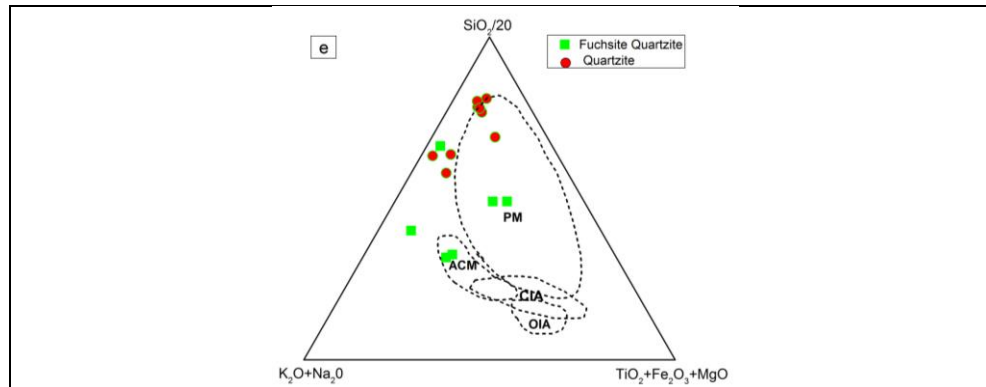
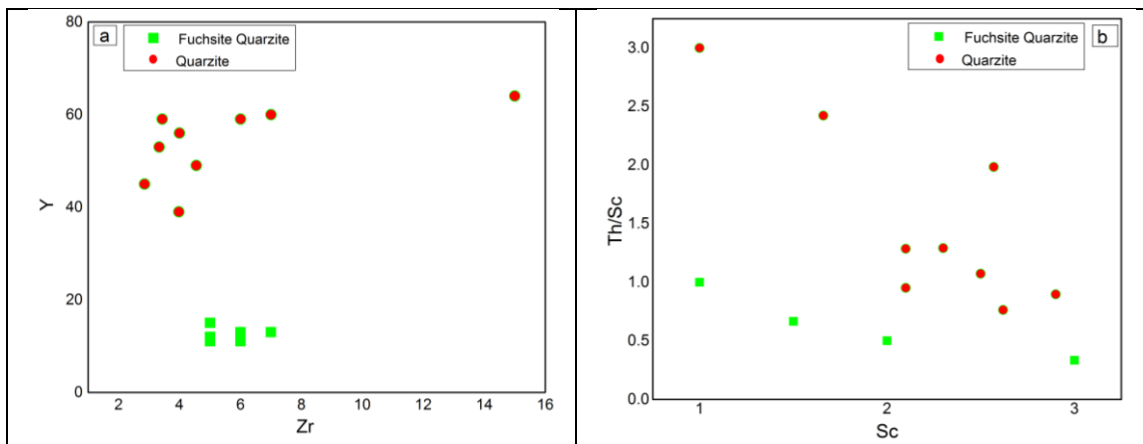


Fig 10: (a) The studied samples fall close to the passive margin tectonic setting as seen in the plot of $\text{Fe}_2\text{O}_3 + \text{MgO}$ vs. $\text{Al}_2\text{O}_3/\text{SiO}_2$ (Bhatia [17]). (b) $\text{Fe}_2\text{O}_3+\text{MgO}$ vs. TiO_2 plot was used for depicting the tectonic setting of studied quartzites (Bhatia, [17]). (c) $\text{K}_2\text{O}/\text{Na}_2\text{O}$ vs SiO_2 plot of quartzites depicting predominant passive margin setting (Roser and Korsch, [36]). (d) Ternary diagram $\text{CaO}-\text{N}_2\text{O}-\text{K}_2\text{O}$ (Bhatia [17]); (e) $\text{SiO}_2/20-\text{K}_2\text{O} +\text{Na}_2\text{O}-\text{TiO}_2 +\text{Fe}_2\text{O}_3(\text{t})+ \text{MgO}$ (Kroonberg, [37]) Ternary plot showing most of the samples of these units fall in a passive margin setting; OIA-Oceanic Island Arc; CIA-Continental Island Arc; PM-Passive Margin; ACM-Active Continental Margin

Trace element compositions of quartzite are presented in Table-2. The plot of Zr vs. Y variation diagram, in which samples of the quartzite cluster separately (Fig. 11a). The samples of Quartzites show a high Zr/Y value range from 4.27 to 17.20, while fuchsite quartzites display a low value range from 1.83 to 3.0. A positive correlation is observed between Th/Sc vs. Sc plot for the studied quartzites (Fig.11b). The binary plots Eu/Eu^* versus Zr/Y, Th/Sc, and (La/Sm) N illustrate the scattering distribution of all studied samples. On binary plots, the quartzite samples are plotted Eu/Eu^* vs. Zr/Y, Eu/Eu^* vs. Th/Sc, and Eu/Eu^* vs. (La/Sm) N, which depicts that all the samples have scattered patterns. (Fig. 11c, d & e). Thus, using the major and trace elements along with discriminate functions, the data suggests that the samples studied in the area were formed by passive margin tectonics.



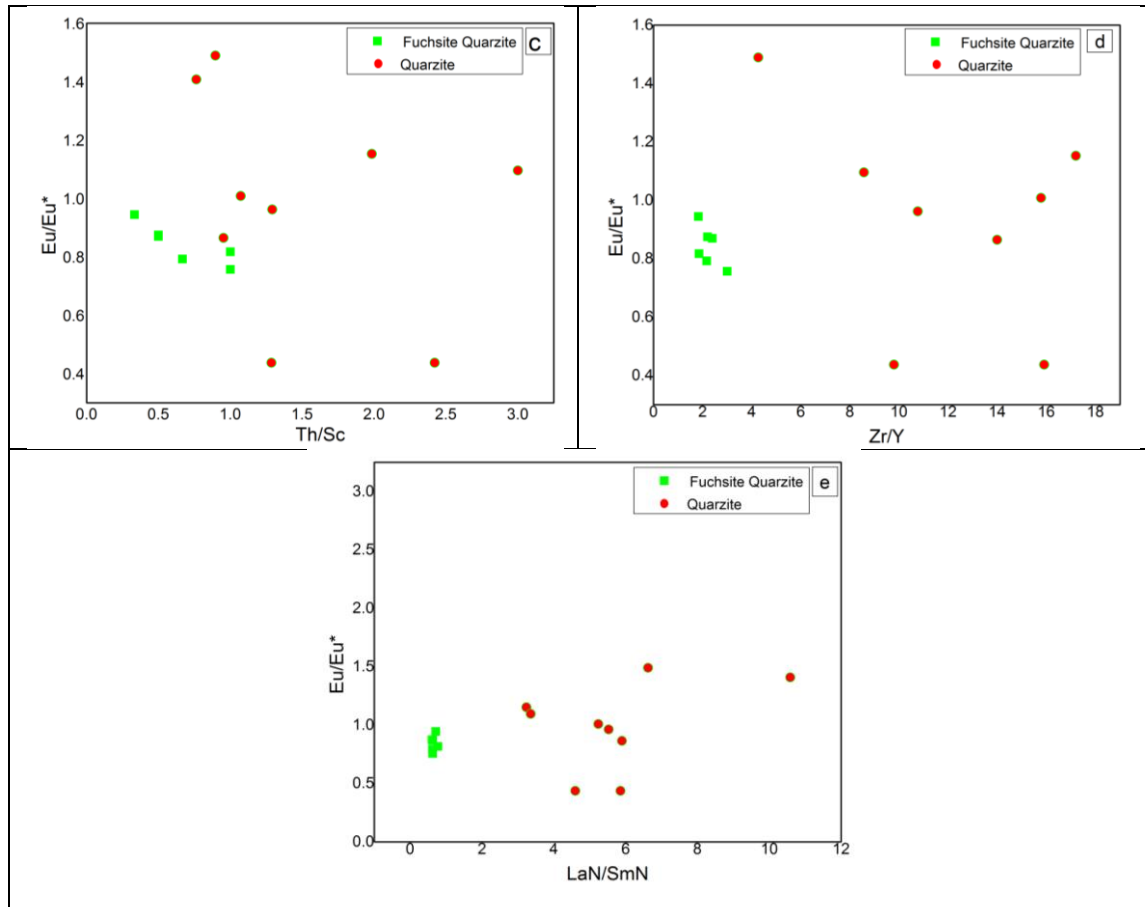


Fig 11: Trace element variation diagrams; (a) Zr vs. Y, (b) Sc vs. Th/Sc, (c) Zr/Y vs. Eu/Eu^* , (d) Th/Sc vs. Eu/Eu^* , (e) La_N/Sm_N vs. Eu/Eu^*

11. CONCLUSION

Geochemical analysis of the studied quartzites shows that they have been subjected to moderate to severe chemical weathering. Different chemical indices, such as the CIW, CIA, and PIA, demonstrate moderate to intense chemical weathering under semi-humid climatic conditions for quartzite and semi-arid to semi-humid conditions for fuchsite quartzite. Based on the petro graphical and geochemical studies, it shows that the quartzite samples are classified as sub-arkose to sub-litharenite. In contrast, the fuchsite quartzite samples are classified as arkose to litharenite. In accordance with the major oxides data, trace element data, and REE data, it seems that the studied quartzites have been mainly the source of felsic igneous rocks with minor contributions from mafic rocks. Using discrimination function diagrams, geochemical data show that studied samples are part of a quartzose sedimentary field. As indicated by the Th/Sc vs Sc diagram, studied quartzites and fuchsite quartzites are located close to sandstone and granite, and are distant from basalt, andesite, and komatiite. In addition, the trace element signatures of

the suspected source materials have also been confirmed by their trace elemental signatures, which include high levels of La, Ce, Th/Sc, La/Sc, Zr/Sc, and Cr/Th ratio.

Geochemical data indicate that the studied fuchsite quartzite and quartzite are of mixed provenance. Additionally, tectonic plot studies show quartzite and fuchsite quartzite were deposited along a passive margin, excluding a few samples on the active margin. The REE profile shows that the sediments were probably derived from a mix of felsic and mafic terrains associated with Archaean metavolcanic terrain enriched with LREE and a slight negative Ce anomaly, as well as flat HREE and a slight negative Eu anomaly. It is concluded from this that the major element ratios ($\text{SiO}_2/\text{Al}_2\text{O}_3$, $\text{K}_2\text{O}/\text{Na}_2\text{O}$), trace elements, and normalized REE patterns indicate that these quartzites are predominantly derived from felsic and mafic sources.

Acknowledgements

Authors are thankful to the Chairman, Department of Applied Geology, and Kuvempu University for extending support to carry out the present research work. We are highly thankful to the Director, WIHG, and Dehradun for providing an opportunity to carryout geochemical analyses. We would like to express our sincere gratitude to everyone who helped and supported this work and to the editor and reviewers for their valuable comments.

References

- 1) M.R. Bhatia and K.A. Crook, "Trace Element Characteristics of Graywackes and Tectonic Setting Discrimination of Sedimentary Basins," *Contributions to Mineralogy and Petrology*, vol. 92, pp. 181–193, 1986, doi:10.1007/BF00375292
- 2) B.P. Roser and R.J. Korsch, 1988, "Provenance Signatures of Sandstone-Mudstone Suites Determined Using Discriminant Function Analysis of Major-Element Data." *Chemical Geology*, vol. 67, pp. 119–139, 1988, doi:10.1016/0009-2541(88)90010-1
- 3) S.R. Taylor and S.M. McLennan, "The Continental Crust: Its Composition and Evolution". Blackwell Scientific, Oxford, pp. 312, 1985.
- 4) S.M. McLennan, "Rare Earth Elements in Sedimentary Rocks: Influence of Provenance and Sedimentary Processes," In: Lipin, B.R. and McKay, G.A.(eds.), *Geochemistry and Mineralogy of Rare Earth Elements*, Vol. 21: Reviews in Mineralogy. The Mineralogical Society of America, pp. 169–200, 1989, doi:10.1515/9781501509032-010
- 5) H.W. Nesbitt and G.M. Young, "Prediction of Some Weathering Trends of Plutonic and Volcanic Rocks Based on Thermodynamic and Kinetic Considerations," *Geochimica et Cosmochimica acta*, vol. 48, pp. 1523–1534, 1984, doi:10.1016/0016-7037(84)90408-3
- 6) C.M. Fedo, H. Wayne Nesbitt, and G.M. Young, "Unraveling The Effects of Potassium Metasomatism in Sedimentary Rocks and Paleosols, with Implications for Paleoweathering Conditions and Provenance," *Geology*, vol. 23, pp. 921–924, 1995, doi:10.1130/0091-7613(1995)023%3C0921:UTEOPM%3E2.3.CO;2
- 7) S. Argast and T.W. Donnelly, "Compositions and Sources of Metasediments in the Upper Dharwar Supergroup, South India," *The Journal of Geology*, vol. 94, pp. 215–231, 1986, doi:10.1086/629024
- 8) P.N. Taylor, B. Chadwick, S. Moorbath, M. Ramakrishnan and M.N. Viswanatha, "Petrography, Chemistry and Isotopic Ages of Peninsular Gneiss, Dharwar Acid Volcanic Rocks and The Chitradurga Granite with Special Reference to The Late Archaean Evolution of the Karnataka Craton, Southern India," *Precambrian Research*, vol. 23, pp. 349–375, 1984, Doi:10.1016/0301-9268(84)90050-0

- 9) A.P. Nutman, B. Chadwick, M. Ramakrishnan and M.N. Viswanatha, "SHRIMP U-Pb Ages of Detrital Zircon in Sargur Supracrustal Rocks in Western Karnataka, Southern India," *Journal Geological Society of India*, vol. 39, no. 5, pp. 367–374. 1992,
- 10) B.P. Radhakrishna and C. Sreenivasaiya, "Bedded Barytes from the Precambrian of Karnataka," *Journal Geological Society of India*, vol. 15, no. 3, pp. 314–315, 1974.
- 11) M.N. Viswanatha, M. Ramakrishnan and T.R. Narayanan Kutty, "Possible Spinifex Texture in a Serpentine from Karnataka," *Journal Geological Society of India*, vol. 18, no. 4, pp. 194–197. 1977.
- 12) B.L. Narayana and S.M. Neqvi, "Geochemistry of Spinifex-Textured Peridotitic Komatiites from Ghattihosahalli, Karnataka, India," *Journal Geological Society of India*, vol. 21, pp. 194–198, April 1980.
- 13) S. Paranthaman, "Geology and Geochemistry of Archaean Ghattihosahalli Mafic-Ultramafic Complex, Chitradurga, Karnataka," *Journal Geological Society of India*, vol. 66, no. 4, pp. 653–657, November 2005.
- 14) T. Hokada, K. Horie, M. Satish Kumar, Y. Ueno, A. Nasheeth, K. Mishima, and K. Shiraishi, "An Appraisal of Archaean Supracrustal Sequences in Chitradurga Schist Belt, Western Dharwar Craton, Southern India," *Precambrian Research*, vol. 227, pp. 99-119, 2013, doi:10.1016/j.precamres.2012.04.006
- 15) M.R. Bhatia, "Petrology, Geochemistry and Tectonic Setting of Some Flysch Deposits," Ph.D. Thesis, The Australian National University., Canberra., 1981.
- 16) S.M. McLennan, S. Hemming, D.K. McDaniel and G.N. Hanson, "Geochemical Approaches to Sedimentation, Provenance, and Tectonics," In: J.J. Mark and Abhijit Basu, (eds.), *Processes Controlling the Composition of Clastic Sediments*. Geological Society of America, Special Paper, vol. 284, pp. 21–40, 1993.
- 17) M.R. Bhatia, "Plate Tectonics and Geochemical Composition of Sandstones," *The Journal of Geology*, vol. 91, pp. 611–627, 1983, doi:10.1086/628815
- 18) F.J. Pettijohn, P.E. Potter and R. Siever, "Sand and Sandstone," Springer Verlag, Berlin, pp. 618 p, 1972.
- 19) M.M. Herron, "Geochemical Classification of Terrigenous Sands and Shales from Core or Log Data," *Journal of Sedimentary Petrology*, Vol. 58, no. 5, pp. 820-829. September, 1988. Doi:10.1306/212F8E77-2B24-11D7-8648000102C1865D
- 20) K.A. Crook, "Lithogenesis and Geotectonics: The Significance of Compositional Variation in Flysch Arenites (Graywackes)," In: R.H. Dott Jr, and R.H. Shaver (eds.), *Modern and Ancient Geosynclinal Sedimentation*. SEPM Society for Sedimentary Geology, SEPM Special Publication, vol. 19, pp. 304–310, 1974.
- 21) R. Cox, D.R. Lowe and R.L. Cullers, "The Influence of Sediment Recycling and Basement Composition on Evolution of Mudrock Chemistry in The South-Western United States," *Geochimica et Cosmochimica Acta*, vol. 59, pp. 2919–2940, 1995, doi:10.1016/0016-7037(95)00185-9
- 22) C. Srinivasaiah, V.N. Vasudev and N.V. Chalapathi Rao, "Tungsten, Barium and Base Metal Mineralization in a Layer of Amphibolite in Mesoarchaean Ghattihosahalli Belt, Western Dharwar Craton, Karnataka, India," *Journal Geological Society of India*, vol. 86, pp. 648–656, 2015, doi:10.1007/s12594-015-0356-7
- 23) T. C. Devaraju, M. M. Raith, B. Spiering, "Mineralogy of the Archean Barite Deposit of Ghattihosahalli, Karnataka, India," *The Canadian Mineralogist*, vol. 37, no. 3, pp. 603–617, 1999.

- 24) M.M. Raith, T.C. Devaraju and B. Spiering, "Paragenesis and Chemical Characteristics of the Celsian-Hyalophane-K-feldspar Series and Associated Ba-Cr Micas in Barite-Bearing Strata of the Mesoarchaeon Ghattihosahalli Belt, Western Dharwar Craton, South India," *Mineralogy and Petrology*, vol. 108, pp. 153–176, 24 June 2013, doi:10.1007/s00710-013-0303-5
- 25) R.L. Cullers, S. Chaudhuri, B. Arnold, M. Lee and C.W. Wolf Jr, "Rare Earth Distributions in Clay Minerals and in the Clay-Sized Fraction of the Lower Permian Havensville and Eskridge Shales of Kansas and Oklahoma," *Geochimica et Cosmochimica Acta*, vol. 39, pp. 1691–1703, 1975, doi:10.1016/0016-7037(75)90090-3
- 26) S. Chaudhuri and R.L. Cullers, "The Distribution of Rare-Earth Elements in Deeply Buried Gulf Coast Sediments," *Chemical Geology*, vol. 24, pp. 327–338, 1979, doi:10.1016/0009-2541(79)90131-1
- 27) L. Schiotte, A.P. Nutman and D. Bridgwater, "U-Pb Ages of Single Zircons within Upernavik Metasedimentary Rocks and Regional Implications for The Tectonic Evolution Of The Archaean Nain Province, Labrador," *Canadian Journal of Earth Sciences*, vol. 29, pp. 260–276. 19 September 1991, doi:10.1139/e92-024
- 28) W.R. Dickinson and C.A. Suczek, "Plate Tectonics and Sandstone Compositions" *The American Association of Petroleum Geologists Bulletin*, vol. 63, pp. 2164–2182, 1979, doi:10.1306/2F9188FB-16CE-11D7-8645000102C1865D
- 29) R. Valloni and J.B. Maynard, "Detrital Modes of Recent Deep-Sea Sands and Their Relation to Tectonic Setting: A First Approximation," *Sedimentology*, vol. 28, pp. 75–83, 1981, doi:10.1111/j.1365-3091.1981.tb01664.x
- 30) F.L. Schwab, "Framework Mineralogy and Chemical Composition of Continental Margin-Type Sandstone," *Geology*, vol. 3, pp. 487–490, 1975, doi:10.1130/0091-7613(1975)3%3C487:FMACCO%3E2.0.CO;2
- 31) H.W. Nesbitt, G.M. Young, S.M. McLennan and R.R. Keays, "Effects of Chemical Weathering and Sorting on the Petrogenesis of Siliciclastic Sediments, with Implications for Provenance Studies," *The Journal of Geology*, vol. 104, pp. 525–542, 1996, doi:10.1086/629850
- 32) L.J. Suttner and P.K. Dutta, "Alluvial Sandstone Composition and Palaeoclimate Framework Mineralogy," *Journal of Sedimentary Petrology*, vol. 56, pp. 329–345, 1986, doi:10.1306/212F8909-2B24-11D7-8648000102C1865D
- 33) K. Hayashi, H. Fujisawa, H.D. Holland and H. Ohmoto, "Geochemistry of ~1.9 Ga Sedimentary Rocks from Northeastern Labrador, Canada," *Geochimica et Cosmochimica Acta*, vol. 61, pp. 4115–4137, 1997, doi:10.1016/S0016-7037(97)00214-7
- 34) P.A. Floyd, J.A. Winchester, and R.G. Park, "Geochemistry and Tectonic Setting of Lewisian Clastic Metasediments from the Early Proterozoic Loch Maree Group of Gairloch, NW Scotland," *Precambrian Research*, vol. 45, pp. 203–214, 1989, doi:10.1016/0301-9268(89)90040-5
- 35) T.C. Devaraju and K.S. Ananthamurthy, "Mineralogy of the Fuchsites from Gattihosahalli, Chitradurga District," *Indian Academy of Sciences Proceedings: Earth and Planetary Sciences*, Vol. 87 A, No. 11, November 1975, pp. 255-261.
- 36) B.P. Roser and R.J. Korsch, "Determination of Tectonic Setting of Sandstone-Mudstone Suites Using SiO₂ Content and K₂O/Na₂O Ratio," *The Journal of Geology*, vol. 94, pp. 635-650, 1986, doi:10.1086/629071
- 37) S.B. Kroonenberg, "Effects of Provenance, Sorting and Weathering on the Geochemistry of Fluvial Sands from Different Tectonic and Climatic Environments," *Proceedings of the 29th International Geological Congress, Part A, Kyoto, Aug. 24–Sep. 3, pp. 69–81, 1994.*

- 38) M. Jayananda, T. Kano, J.J. Peucat and S. Channabasappa, "3.35 Ga Komatiite Volcanism in the Western Dharwar Craton, Southern India: Constraints from Nd Isotopes and Whole-Rock Geochemistry," *Precambrian Research*, vol. 162, pp. 160–179, 2008, doi:10.1016/j.precamres.2007.07.010
- 39) S.M McLennan, "Relationships Between the Trace Element Composition of Sedimentary Rocks and Upper Continental Crust," *Geochemistry Geophysics Geosystems*, vol. 2, pp. 154-155, 2001, doi:10.1029/2000GC000109
- 40) K.C. Condie, "Chemical Composition and Evolution of the Upper Continental Crust: Contrasting Results from Surface Samples and Shales," *Chemical Geology*, vol. 104, pp. 1–37, 1993, doi:10.1016/0009-2541(93)90140-E
- 41) M.R. Bhatia, "Rare Earth element Geochemistry of Australian Paleozoic Graywackes and Mudrocks: Provenance and Tectonic Control," *Sedimentary Geology*, vol. 45, pp. 97–113, 1985, doi:10.1016/0037-0738(85)90025-9
- 42) H.W. Nesbitt and G.M. Young, "Early Proterozoic Climates and Plate Motions Inferred from Major Element Chemistry of Lutites," *Nature*, vol. 299, pp. 715–717, 1982, doi:10.1038/299715a0
- 43) R.L. Cullers, Abhijith Basu and L.J. Suttner, "Geochemical Signature of Provenance in Sand-Size Material in Soils and Stream Sediments near The Tobacco Root Batholith, Montana, U.S.A.," *Chemical Geology*, vol. 70, no. 4, pp. 335-348, 30 September 1988, doi:10.1016/0009-2541(88)90123-4
- 44) R.L. Cullers, "The Geochemistry of Shales, Siltstones and Sandstones of Pennsylvanian-Permian Age, Colorado, USA: Implications for Provenance and Metamorphic Studies," *Lithos*, vol. 51, pp. 181-203, 2000, doi:10.1016/S0024-4937(99)00063-8
- 45) R.L. Cullers and V.N. Podkovyrov, "Geochemistry of the Mesoproterozoic Lakhanda Shales in Southeastern Yakutia, Russia: Implications for Mineralogical and Provenance Control, And Recycling," *Precambrian Research*, vol. 104, pp. 77–93, 24 May 2000, doi:10.1016/S0301-9268(00)00090-5